LA-UR- 99-2490

Approved for public release; distribution is unlimited.

Title: NEAR-FIELD ATMOSPHERIC DISPERSION AROUND COMPLEX OBSTACLES USING A 3-D TURBULENT FLUID-FLOW MODEL

Author(s): Bruce C. Letellier, TSA-11
Louis Restrepo, OMICRON

Submitted to: 1999 Safety Analysis Workshop
June 13–18, 1999
Portland, OR

Near-Field Atmospheric Dispersion Around Complex Obstacles Using a 3-D Turbulent Fluid-Flow Model

Bruce Letellier
Los Alamos National Laboratory
Los Alamos, NM
(505)665-5188
bcl@lanl.gov

Louis Restrepo
Omicron Safety and Risk Technologies, Inc.
Albuquerque, NM
(505)883-0553
lrestrepo@ibm.net

ABSTRACT

A recent safety analysis effort at Los Alamos National Laboratory involved a postulated release of fission products from the ventilation system of a large building located near the wall of a very narrow canyon. At immediate exposure risk from this type of accident are security personnel stationed within 50 and 150 m of the building. Operational experience with wind patterns in this area suggested that a turbulent-flow model might be needed to effectively describe near-field dispersion for the purpose of estimating exposure and inhalation doses from radionuclides.

The FLOW-3D® fluid model (Flow Science, Inc., Los Alamos, New Mexico) provides a general capability for finding three-dimensional, time-dependent, Navier-Stokes solutions to fluid-transport problems in a wide variety of aerodynamic and hydrodynamic design/analysis applications. This code provides boundary conditions such as constant or time-dependent directional flows, obstacle properties such as roughness and heat generation, and transport mechanisms such as particulate settling and diffusion that are necessary for facility-safety consequence analyses.

FLOW-3D® was used successfully to model turbulent wind fields in an idealized geometry consisting of the reactor facility sitting in a niche against a canyon wall and to predict downwind air concentrations for a puff of tracer material released from the top of the building. Resolutions of approximately 1 m were applied in a graduated spatial grid containing approximately 125,000 cells over the domain of interest. Steady-state solutions for uniformly incident winds and transport of unit-concentration tracer sources were accomplished in less than 45 CPU hours on a 450-MHz desktop computer. Details of the methodology used for these calculations and color animations of puff dispersion in the complex wind field surrounding the building wake are presented.

Comparisons of plume-averaged concentrations predicted by FLOW-3D® near a single building placed in a uniform wind field were made with available correlations for this simple configuration to illustrate the performance of the numerical model in contrast to a more conventional approach. Agreement within a factor of 2–3 was obtained under all conditions for this gross concentration metric. Point concentrations predicted near the ground by FLOW-3D® are conservatively overestimated by assuming uniform mixing within the building wake.

The practical application of state-of-the-art turbulent-fluid modeling tools can help broaden our understanding of the interactions between source geometries, wind fields, and large obstacles for the difficult safety analysis problem of near-field atmospheric dispersion in complex configurations of buildings and terrain features. This provides a much-needed transition from realistic transport effects near the source to our common intuition of long-range Gaussian dispersion. As experience with fluid-dynamic models grows, they will provide a defensibly conservative, yet realistic, means of estimating health consequences for on-site, co-located workers.

1.0. Introduction

The critical assembly facility at Los Alamos National Laboratory features the enriched-uranium, fast-burst Godiva IV machine, which is housed in a large building known as Kiva III. Recent security upgrades now permit personnel access within 50 m during operation of the reactor, and potential exposure of these individuals to fission products released during a postulated design-basis accident became the subject of an unresolved safety question determination issued by the Department of Energy (DOE). The Los Alamos Probabilistic Risk and Hazard Analysis Group (TSA-11) was tasked to independently evaluate the adequacy of the existing accident analysis provided in the facility Safety Analysis Report (SAR) (Ref. 1).

Estimation of near-field consequences from atmospheric dispersion of fission products at Kiva III is complicated by the presence of large obstacles such as the building itself, thick stands of fir trees, and a very steep canyon wall. Turbulent eddies and streamlines around these features can introduce local variations in air concentration that are not represented adequately by the standard Gaussian diffusion model, and empirical correlations for building-wake dispersion are only available for a limited set of building geometries and wind conditions. To address these difficulties, a computational fluid dynamics (CFD) model called FLOW-3D® (Ref. 2) was used to compute steady-state wind patterns and fission-product plume trajectories within 200 m.

This paper presents the methodology and assumptions used to perform calculations of the complex wind fields surrounding the building wake and to disperse puff releases of tracer material. Contours of wind velocity and puff-dispersion animations illustrate the type of information that can be obtained relatively easily from a CFD model. Air-concentration histories for the puff (observed at selected receptor locations) were ultimately integrated with time-dependent source terms to estimate total exposures over the duration of an accident scenario; however, a discussion of the source term and dose evaluation is provided in a separate paper.

Because of the unfamiliarity of detailed CFD modeling in the safety analysis community, the performance of FLOW-3D® is compared with that of recent correlations for building-wake concentration for the simple configuration of a rectangular obstacle placed in free-field wind conditions. This comparison should not be considered a "benchmark" evaluation of the numerical model because the correlations were derived from wind-tunnel data not immediately available to this study. Nevertheless, it is reassuring to find good agreement between the methods under the assumption of uniform mixing within the recirculation cavity. Here, we rely on the pedigree of the FLOW-3D® model and its history of successful application to diverse industrial research problems to accurately describe complex transport phenomena in the near-field building wake. Details in the wind field and plume development evident in the simulation provide valuable insights regarding appropriate application of the more familiar wake-transport correlations.

2.0. Complex-Wind-Field Calculations

2.1. Modeling Assumptions

Although a great deal of fidelity may be built into a FLOW-3D® calculation, the results can become overly dependent on assumptions made for the boundary conditions. It is more appropriate that a problem be stylized using simplifying assumptions that preserve conservatism while retaining essential features. For example, these calculations ignored the presence of large fir trees immediately upwind of the building to minimize the size of the effective wake, and all surfaces were treated as frictionless to minimize ground-level turbulence. Given an air temperature of 20°F and a symmetry plane placed at the top

boundary to suppress vertical dispersion, these conditions approximate F-class stability with ground-level, night-time drainage flows.

The assumptions applied to generate wind fields tend to confine the plume and are considered conservative because maximum air concentrations at the selected downwind distances were used for dose assessment regardless of actual location above the ground. The true range of boundary conditions, which includes obliquely incident winds and gusting, are not characterized well enough to allow prediction of point concentrations with the degree of defensibility required for safety analyses.

The terrain and obstacles established for these calculations are shown in Fig. 1. With the building center placed at the origin, the domain extends 213 m (700 ft) upwind and 213 m downwind along the canyon and 152 m (500 ft) out into the almost-flat drainage basin. The canyon wall rises 15 m (50 ft) over a 76-m (250-ft) run and features a slight depression that shelters the Kiva from prevailing winds that blow up and down the canyon to the east and west. The building is sheltered further in an excavated niche that leaves only a 4-m (13-ft) channel for air flow. Figure 2 shows the computational grid that was imposed on the X-Y directions of the domain. A similar grid, which places the highest spatial resolution near the building, is defined in the Z direction. Approximately 125,000 cells were used in this model with spatial resolutions near the building on the order of 1 m or less in each dimension.

Constant-velocity boundary conditions of 2 and 10 m/s were enforced on each end of the domain, and symmetry planes were defined on the top and both sides. Steady-state turbulent wind fields were established by gradually increasing the boundary velocities from zero to the desired magnitude and then monitoring the average turbulent kinetic energy in the domain until minor oscillations had damped. Among the several options offered by FLOW-3D®, these calculations invoked a k - ε turbulence model to conserve advective momentum between cells. Also, it was found useful to apply an initially lax and then progressively tighter criterion on pressure convergence in order to speed the approach to steady-state flows at the desired incident velocities. Each steady-state field was obtained after approximately 30 to 50 h of CPU time on a 450-MHz desktop computer. Significant reductions in this calculation time are expected with increased experience.

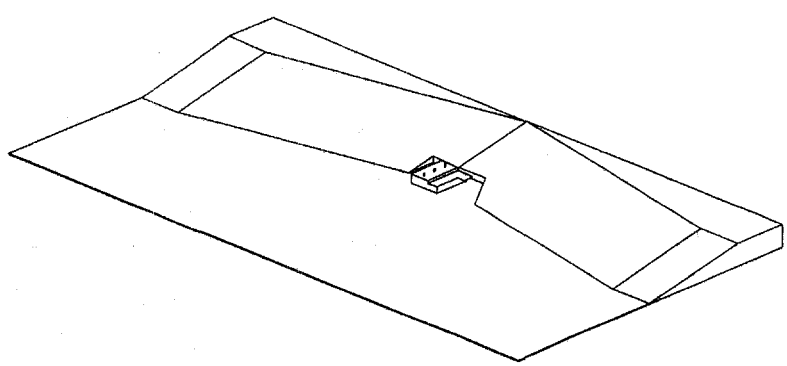

Fig. 1. Stylized terrain and building obstacles present in the FLOW-3D® computational domain. All edges on the building were forced by nodalization mesh planes including three 1-m^3 HVAC vents on top and a very thin extended delivery shelter on the front.

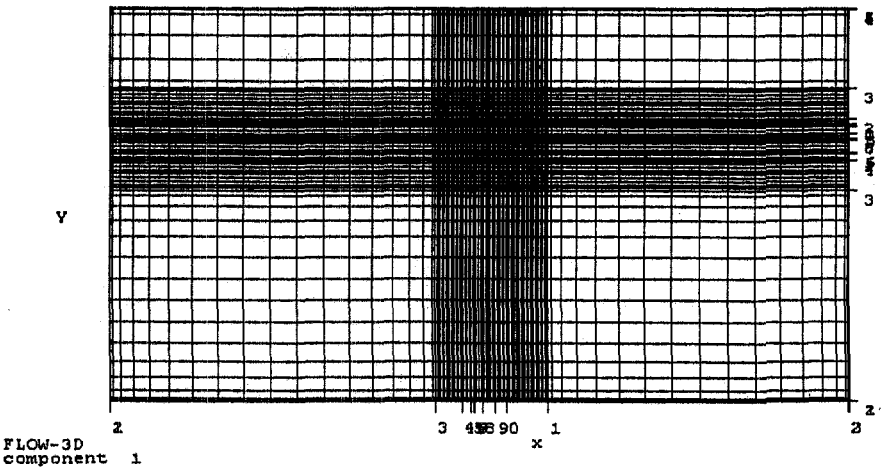

Fig. 2. Graduated rectilinear spatial nodalization in the X-Y plane used for FLOW-3D® computational domain. Approximately 125,000 cells define the region with resolutions of less than 1 m^3 near the building.

2.2. Steady-State Wind-Field Results

Figure 3 shows the type of wind-field detail that can be predicted by FLOW-3D®. Velocity components in the X direction at a height of 9.7 m are shown in color-shaded contours. Positive flow is defined toward the right, so regions in blue indicate flow reversal resulting from turbulent recirculation. The width and extent of the building wake are clearly marked by the separation flows around upstream corners and by the downstream region of reduced velocities. Yellow regions indicate a return to the free-field boundary conditions of 2 m/s, whereas red regions indicate flow acceleration around the building. Acceleration possibly is enhanced artificially in this example because of the presence of the upper boundary condition. This cross section of the wind field, taken at a height near the top of the Kiva, also shows the asymmetry introduced by the presence of the delivery shelter on one side.

Another cross section of the wind field, taken at a height of 2 m, is shown in Fig. 4. The effects of the excavated niche behind the building are evident in the blue regions denoting flow reversal. In fact, the wake cavity is skewed because of the presence of the hillside. The existence of high velocities near the ground in the narrow passage behind the Kiva was confirmed qualitatively by facility staff who frequently walk around the building through relatively calm regions near the front corner into heavy gusts near the back.

A vertical cross section of the wind field is shown in Fig. 5. Again, contour colors denote the X-component of total velocity. Vector lengths and directions show acceleration on the upwind face of the building and recirculation in the wake cavity. Incident winds and flow acceleration create pressure differentials that draw air through the building. Similar FLOW-3D® calculations were performed to determine the exfiltration rate of fission products out of ventilation ducts on top of the building (Ref. 3). Previous analyses had assumed that a downdraft would be created inside by large openings at the top and that primary leak paths existed through smaller gaps and penetrations around doors at ground level (Ref. 4).

A qualitatively similar wind field as that shown in Figs. 3–5 is obtained for 10-m/s boundary conditions, although the regions of flow acceleration around building are enhanced and the recirculation wake is deeper.

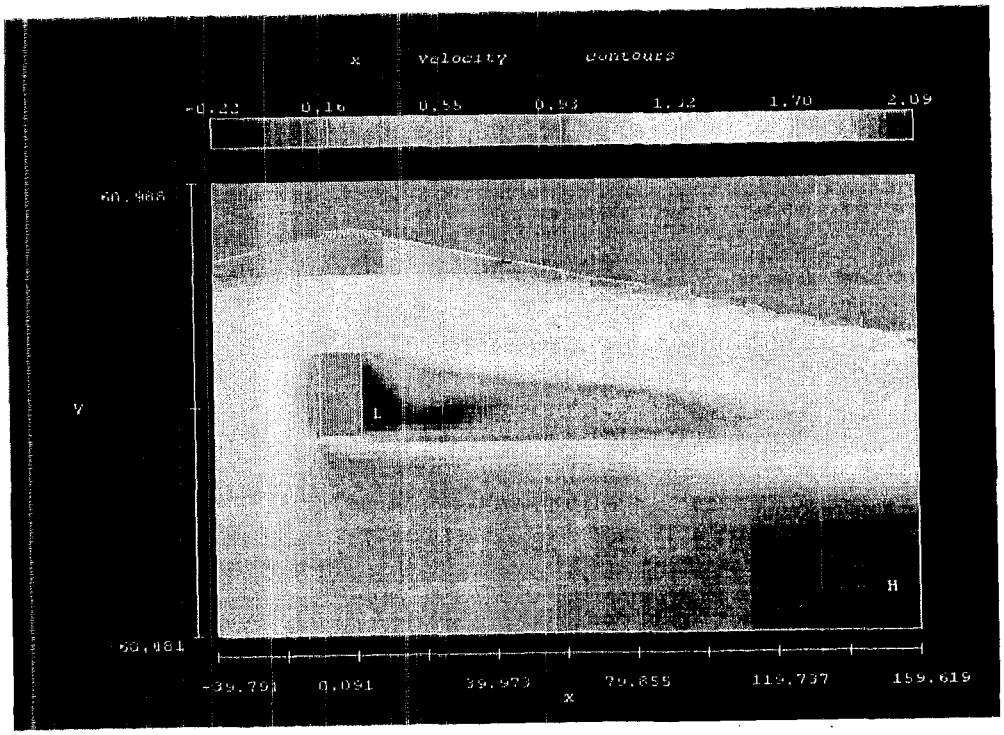

Fig. 3. X components of wind vectors near the top of the Kiva for a 2-m/s boundary condition. Note that negative velocities, or flow reversals, occur in the wake of the building.

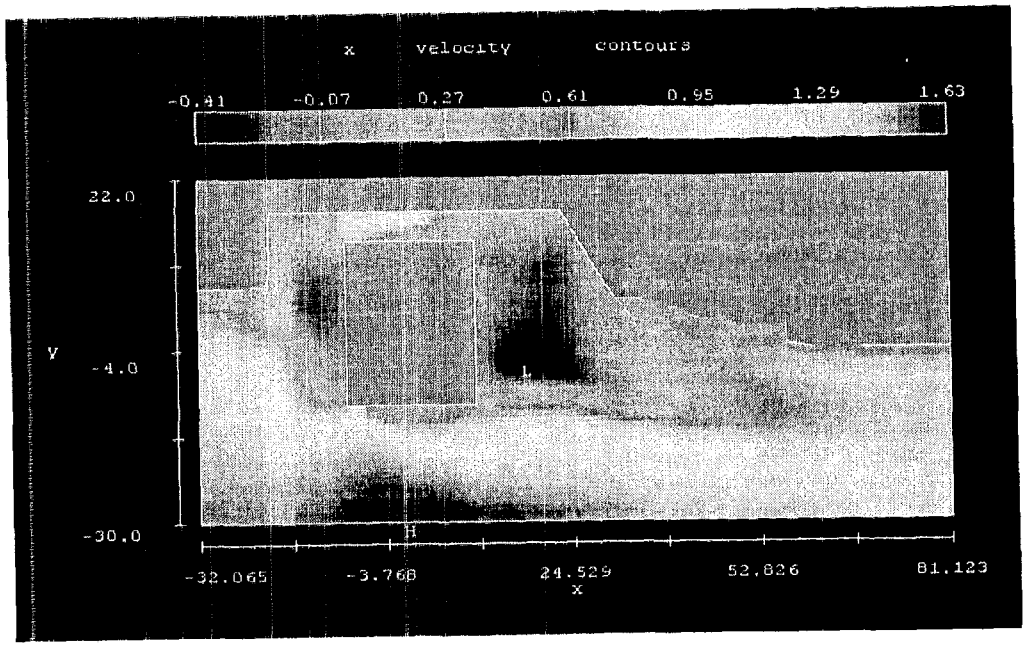

Fig. 4. X components of wind vectors near the ground for 2-m/s boundary conditions. Note the effects of the excavated niche on the recirculation cavity shown in blue for regions of flow reversal.

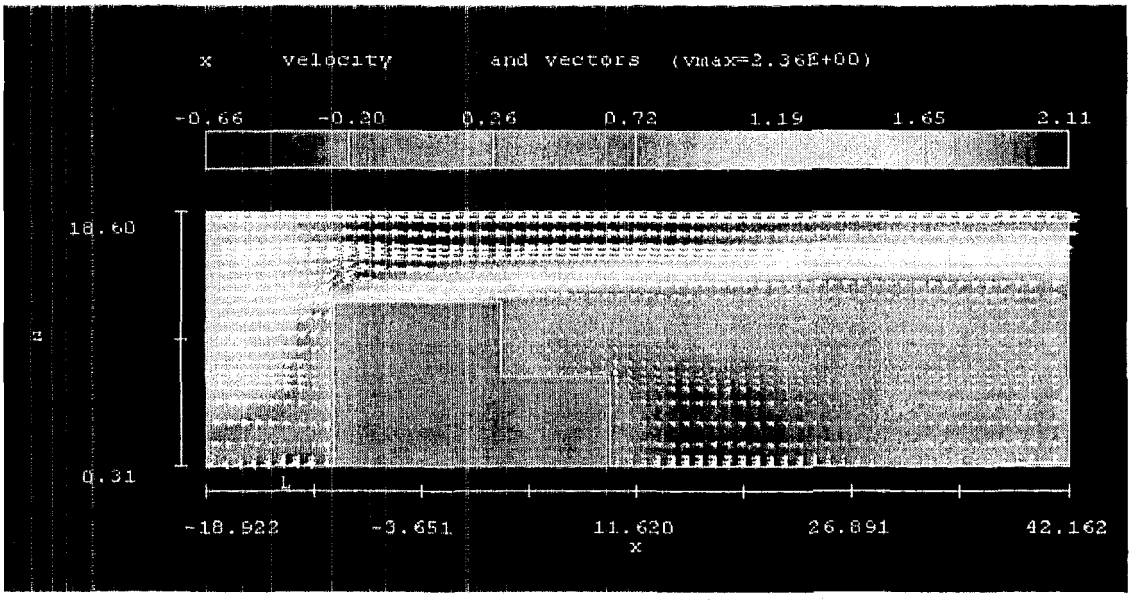

Fig. 4. X components of wind vectors around a vertical cross section of Kiva III for 2-m/s boundary conditions. Lengths of the arrows denote the magnitude of the total velocity. Note the recirculation zones shown in blue where turbulent eddies reverse the flow direction.

3.0. Puff Dispersion

Parametric dispersion calculations were performed by releasing unit-concentration sources into the desired steady-state wind fields from each of the three HVAC vents. Each source had the initial geometry of a 1-m x 1-m x 1-m cube placed at rest just in front of an outlet, but contributions from the three vents quickly merged into a single contiguous plume that followed the streamlines of the wind field. Molecular-diffusion coefficients for the tracer were set to zero so that dilution occurred only through the process of turbulent mixing and transport. Analyses of internal fission-product transport confirmed that material released from the HVAC vents was in small enough aerosol sizes that settling during transport could be ignored, so these calculations assumed a gaseous tracer.

FLOW-3D® computes time-dependent instantaneous concentrations for every cell in the domain. The durations of the dispersion calculations were extended until the bulk of the plumes, as estimated qualitatively by watching relative concentrations, had completely left the domain. Transport times of 10 min were sufficient for 2-m/s winds, and times of 5 min were adequate to track plumes released in 10-m/s winds. Data files of point concentrations on vertical cross sections of the plume were exported from FLOW-3D® for selected downwind locations at 1-s intervals for the first minute and at 10-s intervals thereafter. This information was needed for dose-assessment post processing.

The following figures illustrate the behavior of a single puff released into a steady-state wind field. FLOW-3D® does not currently have the capability to introduce a steady-state concentration source (although, representative aerosol particles can be emitted continuously), but this was not a serious limitation. Because of the time-dependent nature of the fission-product source, each puff representing a discrete time interval of the plume had a different isotopic composition at the time of passage past the receptor location. Thus, the contributions of each plume segment had to be superimposed individually anyway using the proper dose-conversion factors at the time of exposure and the proper mass scalings.

Figure 5 illustrates plume development at 1 min for a single puff of tracer material released into a wind field corresponding to 2-m/s boundary conditions. Note the complex spatial structure that is introduced by the bilevel building configuration. This structure persists up to 200 m downwind before the plume cross section approaches uniform mixing. Turbulent recirculation between building levels and near the base of the Kiva delays the transport of some material in regions of slowly diminishing concentration and may actually increase the effective holdup time available for fission-product decay. The potential for extended holdup time was ignored conservatively in the dose assessment for this facility.

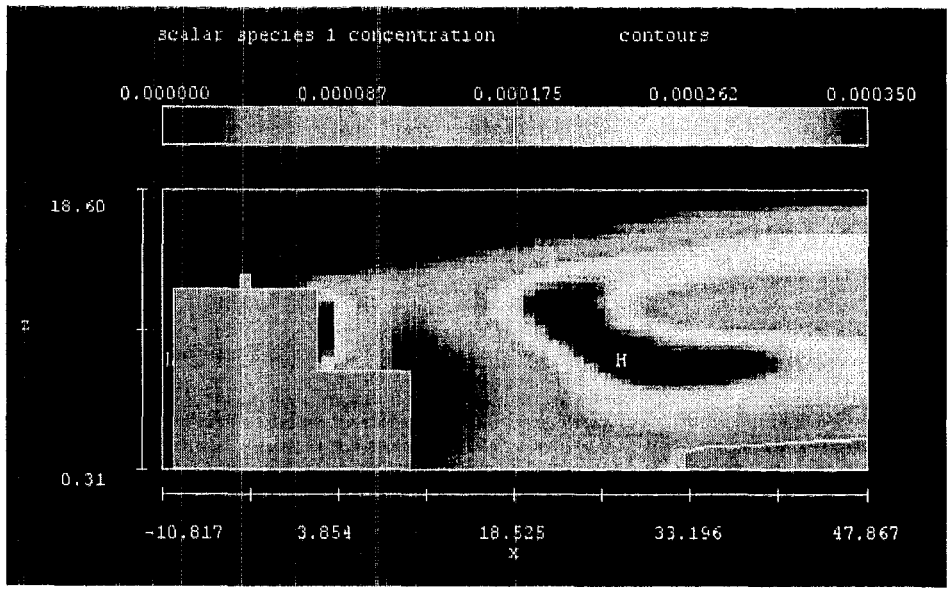

Fig. 5. Air-concentration contours at 1 min. following concurrent release of three unit-concentration puffs (one from each HVAC vent). The accompanying animation illustrates the entire plume development. Note that contours in each frame are scaled to the current maximum concentration to highlight residual holdup in the wake cavity.

A horizontal cross section of the same plume, taken near the ground at 3 min, is shown in Fig. 6. The presence of the sloping hillside skews ground-level flow and perturbs lateral dispersion. In this example, terrain features can potentially channel material closer to one receptor location of concern.

4.0. Performance Comparisons

Turbulent flow patterns and recirculation cavities created near a building can have a significant effect on the downwind transport and dispersion of hazardous materials. Greater confidence can be maintained in the predictions of such phenomena by FLOW-3D® if the code results compare well with measurements, scale tests, or existing "standard" models available for similar release conditions. For this purpose, FLOW-3D® calculations of air concentrations within the wake cavity of a simple rectangular building in free-field wind conditions were compared with those obtained by two recent correlations derived from wind-tunnel data.

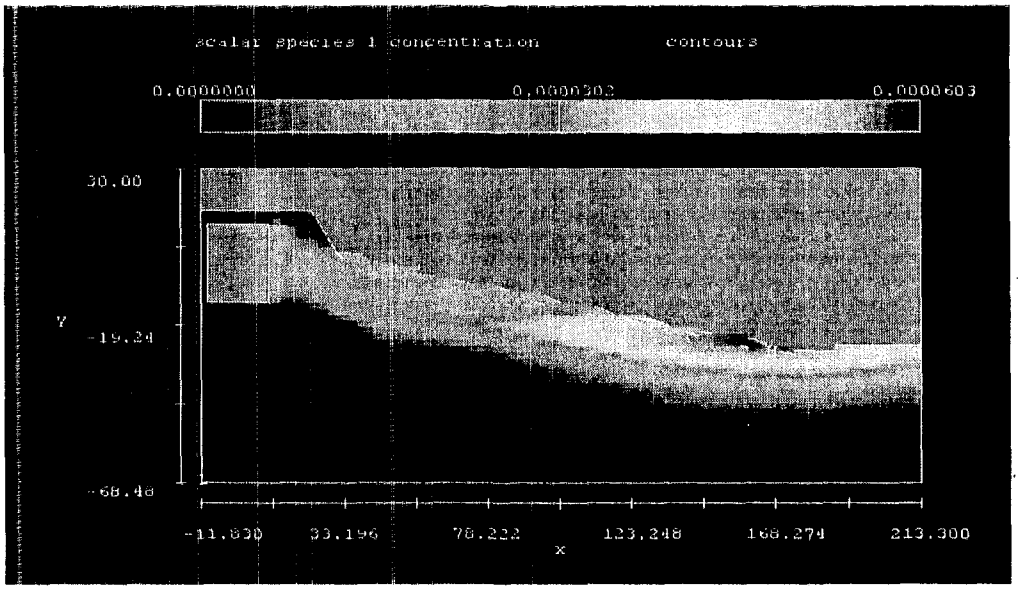

Fig. 6. Air-concentration contours at 3 min following concurrent release of unit-concentration puffs (one from each HVAC vent). The accompanying animation illustrates the entire plume development. Note that contours in each frame are scaled to the current maximum concentration to highlight residual holdup in the wake cavity.

4.1. Analytic Building-Wake Models

Described here are two different analytic models that can be used to estimate ground-level concentrations in the lee-side recirculation cavity of a building from a steady-state release of tracer material. These two models by Wilson and Briggs (Refs. 5–6), respectively, were derived from recent wind-tunnel data reported by Hall (Refs. 7–8). The first was derived primarily to describe concentrations in the recirculation (near-wake) cavity for releases from short stacks where there is an opportunity for some fraction of the total release to become trapped and well mixed (Ref. 9); i.e.,

$$C_V = \frac{f_c Q}{V_0 \left[1 + 13 \left(\frac{T_a}{T_s} \right)^{1/2} \frac{W_0}{u_h} \right] + \frac{u_h x_s^2}{16}}, \tag{1}$$

where C_V is the air concentration {kg/m^3}, f_c is the fraction of the material released that is trapped or captured in the recirculation cavity, $1 - f_c$ is the fraction that rises above the turbulent wake of the building and is subject to downwash effects, Q is the release rate from the building {kg/s}, W_0 is the initial plume speed {m/s}, V_0 is the initial volumetric flux {m^3/s}, x_s is the distance from the release location to the receptor {m}, u_h is the wind speed at the release point {m/s}, and the temperatures T_a and T_s {K} refer to the ambient air and the plume exhaust, respectively.

The second model was developed to describe ground-level concentrations in the far wake beyond the recirculation region. This equation was derived originally for buoyant plumes emitted uniformly from the building face. Again, this correlation is strictly appropriate only to the wake region where the release segment or plume has become well mixed. The form of the second equation is

$$C_V = \frac{f_c Q \exp\left(-6F_{**}^{0.4}\right)}{u_h R^2 \left[0.037 + 0.03\left(\frac{x_s}{H_b}\right)^2 + F_{**}^2\left(\frac{x_s}{H_b}\right)^2 + \left(\pi \frac{\sigma_y \sigma_z}{R^2}\right)^3\right]^{1/3}}, \quad (2)$$

where $R = H_b^{2/3} W_b^{1/3}$ is the building scaling length {m} with H_b and W_b defined as the building height and width {m}, respectively. The crosswind dispersion parameter σ_y {m} is defined by the relation $\sigma_y = a x_s^b$ and the vertical dispersion parameter σ_z {m} is defined by the relation $\sigma_z = c x_x^{\ d} + e$ (Ref. 10), where the dispersion coefficients *a, b, c, d* and *e* are given in Table 1 for selected meteorology conditions. The nondimensional buoyant flux $F_{**} = f_c F_0 / u_h^3 W_b$, where $F_0 = g W_0 A_s (T_s - T_a)/\pi T_s$ is the buoyancy flux {m^4/s^3} for gravitational acceleration g {m/s^2} and plume-source cross section A_s {m^2}. The factor $\exp\left(-6F_{**}^{0.4}\right)$ in Eq. (2) represents the lift-off correction factor; for nonbuoyant releases where $F_0 = 0$, this term equals 1.0.

Table 1. Selected dispersion coefficients for crosswind and vertical dispersion parameters $\sigma_y = a x_s^b$ and $\sigma_z = c x_x^{\ d} + e$.

Stability Class	*a*	*b*	*c*	*d*	*e*
B	0.2751	0.9031	0.028	1.149	3.3
F	0.0722	0.9031	0.086	0.74	-0.35

A critical parameter of both models is the fraction, f_c, of the plume that is captured in the building recirculation cavity. This fraction can be crudely estimated by integrating the Gaussian dispersion that would occur between the plume centerline height and the ground if the building were not present. Thus,

$$f_c = \frac{1}{2}\left[1 + \mathrm{erf}\left(\frac{H_b - h_c}{\sqrt{2}\sigma_z'}\right)\right], \quad (3)$$

where erf denotes the error function and h_c is the plume centerline height {m}. In Eq. (3), the vertical dispersion parameter σ_z' {m} is characterized by the correlation $\sigma_z' = 0.21 R^{1/4}(x_b + L_R)^{3/4}$, where x_b is the downwind distance from the source to the building edge {m} and the length of the recirculation cavity $L_R = 1.3 W_b / [1 + 0.25(W_b / H_b)]$ {m}.

4.2. Model Inputs

For the confirmatory analysis, the information given in Table 2 was used to determine the ground-level air concentrations at two different downwind distances that are impacted by the building wake.

Table 2. Values assumed for evaluation of analytic building-wake concentration models.

Property	Assumed Values
Building dimensions	Length = 19.8 m, width = 24.7 m, height = 11.9 m
Emission rate	1 kg/s
Volumetric flow rate	0.795 m^3/s for 2-m/s wind and 3.802 m^3/s for 10-m/s wind
Exhaust speed	0.685 m/s
Receptor locations	45.7 and 152.4 m downwind
Wind speed and stability	2 and 10 m/s for stability classes F and B, respectively
Ambient and release temperature	267 K (20°F)
Distance from release to the downwind edge of building	7 m
Single stack (ventilator) area	1.16 m^2
Trapped release fraction	1.0

FLOW-3D® calculations of steady-state wind fields were generated for 2- and 10-m/s winds perpendicularly incident on the width of the same rectangular building with no surrounding obstacles. Steady-state air concentrations were then computed near the ground at the same receptor distances for a continuous release of unit-concentration tracer material under similar volumetric flow rates. As previously described, the FLOW-3D® boundary conditions accurately represent F-class stability for 2-m/s winds; no adjustments were made to approximate B-class stability except to increase the wind speed. The source geometry used for the simulations matches that in Table 2 except that the source was introduced to the wind field at roof level with no initial velocity, i.e., at rest.

Steady-state air concentrations corresponding to a continuous release were estimated from the FLOW-3D® puff simulation in the following manner. First, digital data of air concentrations on crosswind slices of the plume were archived for every time step at the receptor distances of interest. Because the experimental correlations assume uniform mixing in the building wake, a single spatially averaged concentration was then computed at each time step to smooth local variations. This average included all cells in the plume cross section with nonzero concentrations. The resulting time histories of average concentration passing a point exhibit the smooth increase and decline that one expects on the centerline of an instantaneous Gaussian puff model, except that the tail persists to somewhat longer times due to recirculation in the wake cavity. Finally, the time-dependent average concentrations were integrated over the total observation time to estimate the constant air concentration that would be observed for a continuous plume whose differential components contribute all segments of the puff history simultaneously.

The largest discrepancy between the FLOW-3D® simulations and the analytic wake models lies in the trapped release fraction chosen for the correlations. Wake recirculation is computed automatically by the CFD model, but it is almost impossible to choose *a priori* a realistic value with which to evaluate the correlations. A value of $f_c = 1.0$ is obviously a conservative choice, and it matches well the experimental conditions associated with the correlations; however, when trying to make a reasonable dose assessment for an unusual building configuration and release geometry, one is at a loss for an appropriate choice of this parameter. Results for any value of the trapped release fraction are easily obtained because f_c is a simple scalar parameter.

4.3. Model Results

Table 3 presents the average air concentrations at two receptor distances for the conditions of 2-m/s wind under stability class F and 10-m/s wind under stability class B. These concentrations were calculated based on Eq. (1) for near-wake regions and Eq. (2) for far-wake regions using the information given above in Table 2. In general, the near-wake model gives slightly higher estimates than the far-wake model for the closer receptor under both wind conditions, and the far-wake model is a factor of 1.5 to 4 times higher at farther distances than the near-wake correlation.

Table 3. Ground-level air concentrations predicted using near- and far-field wake-cavity models.

	Concentration (kg/m^3)			
	Near-Wake Model		Far-Wake Model	
Receptor Distance (m)	2 m/s - F	10 m/s - B	2 m/s - F	10 m/s - B
45.7 (150 ft)	3.8E-3	7.6E-4	2.8E-3	4.7E-4
152.4 (500 ft)	3.4E-4	6.9E-5	1.3E-3	1.0E-4

Figure 7 shows plume development at 2 min computed by FLOW-3D® for the test problem under 2-m/s wind conditions. Here again, this figure shows a snapshot of air concentrations that are evolving for a single puff release. The first panel shows a vertical cross section of air concentrations through the building centerline and the second shows a horizontal cross section at roof level. Animations of vertical plume development show that some of the tracer rises above the building and becomes entrained in the free-field winds while some becomes well mixed in the wake after about 3 min. It is difficult estimate visually what fraction is trapped in the recirculation region, but it is clear that material can travel several building widths downwind before being drawn back into the wake. Horizontal concentrations at and above the roof exhibit a striking bifurcation as material is entrained in separation eddies from each corner. This structure persists for almost 6 min after release before uniform mixing of recirculated material begins to dominate the local concentration

A rudimentary attempt was made to quantify the material fraction captured in the FLOW-3D® building wake. Average concentrations at each time step of the puff history were computed using (1) *all* cells with nonzero concentrations, which corresponds to a capture fraction of 1.0 and (2) *only* those cells with nonzero concentration lying below the building height, which assumes that material in the higher cells is entrained in the free-field flow. The ratio of steady-state plume concentrations obtained by these two methods then approximates the capture fraction required to evaluate the building-wake correlations.

Estimates of constant plume-averaged concentrations computed from FLOW-3D® simulations appear in Table 4. Comparisons of this bulk concentration metric with results from the correlations are remarkably close for most conditions. Notice that the near-wake correlations are higher than the simulated results for a close receptor under both conditions and that far-wake correlations are higher or equivalent to the simulated results for a more distant receptor. This is the trend in conservatism that one might expect from two correlations tailored for specific regimes. These comparisons apply between FLOW-3D® concentrations averaged over the full plume cross section.

Estimates of the trapped material fraction given by the ratio of wake-region concentrations to full-plume concentrations are higher than expected from visual observation of plume development. In general, the trapped fraction is larger for higher wind speed and approaches 1.0 for 10-m/s conditions. The ratio of $f_c = 1.2$ in Table 4 reflects the fact that large areas in the upper region of the full plume have low concentrations. When these areas are ignored, the average concentration increases.

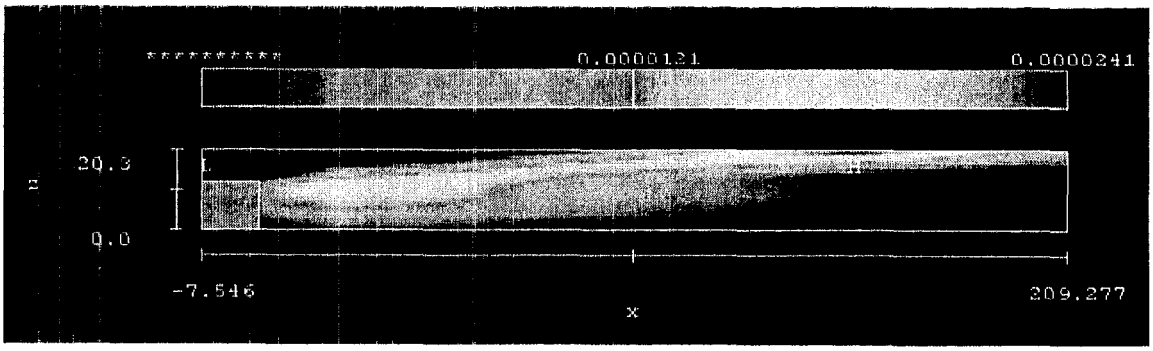

(a)

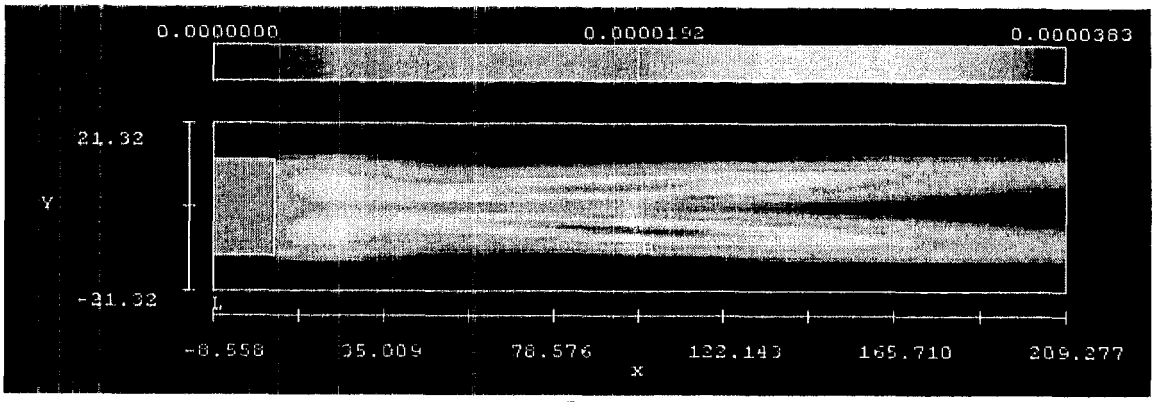

(b)

Fig. 7. Air concentrations in 2-m/s wind conditions at 2 min for a single puff release at the top of the building. Panel (a) shows a vertical cross section through the building midplane. Panel (b) shows a horizontal cross section at roof level. Each frame of the associated animations is scaled to the current maximum concentration.

Table 4. Spatially averaged air concentrations predicted for the test problem using FLOW-3D® for both full plume averaging and partial plume averaging. The ratio approximates the fraction of material trapped in the recirculation wake.

Receptor Distance (m)	2-m/s Winds			10-m/s Winds		
	Conc. (kg/m^3)			Conc. (kg/m^3)		
	Full Plume	Wake	f_c	Full Plume	Wake	f_c
45.7 (150 ft)	1.4e-3	1.2e-3	0.91	2.5e-4	3.0e-4	1.2
152.4 (500 ft)	5.9e-4	4.3e-4	0.73	1.2e-4	1.1e-4	0.96

5.0. Conclusions

This work has demonstrated the utility and practicality of using fluid-dynamic models for near-range dispersion of hazardous materials in the context of a facility-safety assessment. CFD codes predict physical effects beyond the scope of traditional plume and puff models, and they can be equipped with the machinery necessary to treat complicated source terms like time-dependent release rates with fission-

product decay. As with any detailed modeling capability, the approach to realistic, predictive transport methods must be balanced by recognized uncertainty inherent to the boundary conditions so that conservatism appropriate to a safety analysis is maintained.

The introductory comparison presented here between FLOW-3D® simulations of a simple building-wake problem and available analytic approximations lends confidence that CFD tools can be applied to more complex configurations where correlations are not available or not appropriate. For example, the building-wake equations used here are wholly inadequate to treat time-dependent fission-product release. In regard to the performance of the correlations with respect to the simulations, it was found that plume-averaged steady-state concentrations agree remarkably well for the simple test problem. Further investigation of the FLOW-3D® plumes is needed to quantify the trapped release fraction, which is key to obtaining reasonable results from the correlations, and to estimate the degree of conservatism implicit in the assumption of uniform mixing within the wake.

It is not typical to find such a high-level predictive model applied to a safety-analysis evaluation, but FLOW-3D® has proven to be a tractable means of investigating complex wind fields near buildings to generate conservative estimates of personnel dose. We hope that the results and comparisons presented here will initiate the process of familiarization and acceptance of CFD modeling capabilities within the safety analysis community. With further experience and validation, computational tools of this type offer a powerful means to address traditionally difficult issues surrounding exposure of on-site workers to potential health hazards.

References

1. Confirmatory Analysis for Godiva-IV Security-Upgrades USQ," Los Alamos National Laboratory report TSA-11-99-R122 (February 1999).
2. "Flow-3D User's Manual, Excellence in Flow Modeling Software, Version 7.1," Flow Science, Inc., Los Alamos, New Mexico (1997).
3. C. Shaffer, "Leak-Path-Factor Analysis for the Kiva-III Facility Following Godiva-IV Extreme Excursion," Innovative Technology Solutions Corp. report ITS/LANL/KIVA3-99-01 (1999).
4. R. R. Paternoster et al., "Safety Analysis Report for the Pajarito Site (TA-18) and the Los Alamos Critical Experiments Facility (LACEF)," Los Alamos National Laboratory report LA-CP-920235, Rev. 4 (1998).
5. D. J. Wilson, "Numerical Modeling of Dispersion from Short Stacks," Seminar 14, American Society of Heating, Refrigeration, and Air Conditioning, Engineering, Atlanta, Georgia (1995).
6. G. A. Briggs, "Conservative Re-fitting of Lift-off Equation," Unpublished paper, (August 15, 1996).
7. D. J. Hall and R. A. Waters, "Further Experiments on a Buoyant Emission from a Building," Report No. LR 567 PAISBN 0 85624 425 2, Warren Spring Laboratory, Gunnels Wood Road, Stevenage, Hertfordshore SG1 3BX, United Kingdom (1986).
8. D. J. Hall (1995).
9. M. W. Yambert et al., "A Summary of Recent Refinements to the WAKE Dispersal Model, A Component to the HGSYSTEM/UF_6 Model Suite," Oak Ridge National Laboratory report ORNL/TM-13666 (August 1998).
10. Hanna et al. (1982).